SESSION VII

NOBLE GAS SEPARATION

Tuesday, August 8, 19/8
CHAIRMAN: D. Underhill

OPENING REMARKS OF SESSION CHAIRMAN:

At the earlier Air Cleaning Conferences the primary concern with respect to the noble gases was their release during normal and abnormal reactor operation. These papers go beyond this narrow concern, focusing, first, on the radon problem, and secondly, on the recovery of Kr from spent fuel. The fact that these papers deal with problems that are important from the standpoint of workers and general populations physically quite far from the location of nuclear reactors shows, in my opinion, a maturing of the research in nuclear safety.

One paper in this session will deal with radon produced as a product of uranium before it goes into the nuclear fuel cycle and the other deals with recovery of by-product krypton-85 from the offgases after the fuel has been processed through the reactor.

DYNAMIC ADSORPTION OF RADON ON ACTIVATED CARBON

Kaye P. Strong and Desmond M. Levins
Australian Atomic Energy Commission
Research Establishment, Lucas Heights,
Sydney, N.S.W. 2232 Australia.

Abstract

The adsorption of ^{222}Rn from air onto activated carbon was studied over the range 0-55°C. A sharp pulse of radon was injected into an air stream that flowed through a bed of activated carbon. The radon concentration in the exit from the column was continuously monitored using a zinc sulfide α-scintillation flow cell. Elution curves were analysed to determine the dynamic adsorption coefficient and the number of theoretical stages.

Five types of activated carbon were tested and the dynamic adsorption coefficient was found to increase linearly with surface area in the range 1000-1300 m^2g^{-1}. The adsorptive capacity of activated carbon was reduced by up to 30 per cent if the entering gas was saturated with water vapor and the bed was initially dry. If the bed was allowed to equilibrate with saturated air, the adsorptive capacity was too low to be of practical use.

The minimum height equivalent to a theoretical stage (HETS) was about four times the particle diameter and occurred at superficial velocities within the range 0.002-0.02 m s^{-1}. For superficial velocities above 0.05 m s^{-1}, the HETS was determined by the rate of mass transfer. The application of these results to the design of activated carbon systems for radon retention is discussed.

I. Introduction

Three isotopes of radon occur in nature - ^{222}Rn (half-life = 3.8 days) in the uranium-238 decay chain, ^{220}Rn (half-life = 56 s) or thoron from the thorium decay chain, and ^{219}Rn (half-life = 4 s) from the actinium decay chain. Radon isotopes are not a significant radiological hazard in themselves but, because of their mobility as gases, they act as vehicles for dispersal of their alpha-emitting daughters. Radon-222 is the most significant isotope of radon both in terms of occupational exposure in uranium mines and public exposure resulting from its dispersal. The present approach to radon control in underground mines is to reduce the concentration to acceptable levels by forced ventilation. As easily accessible uranium is mined out, there will be a trend towards deeper mines where the technical problems and costs of forced ventilation could be prohibitive. An alternative approach would be to extract the radon from mine air in the vicinity of the working face. An assessment of radon removal processes[1] concluded that adsorption on activated carbon at ambient temperature was the most promising approach in terms of technical feasibility and cost.

This study of radon adsorption on activated carbon was undertaken to obtain more detailed and accurate mass transfer data than are currently available[2]. Specifically, the results are of value in the design of:

- Large scale equipment to remove radon from underground mine air by adsorption at ambient temperature[1,3].
- Gas masks or canisters containing activated carbon for short-term use in atmospheres containing very high radon concentrations

such as unventilated stopes[4].

- Apparatus used in the analysis of ^{222}Rn and ^{226}Ra by methods that involve the collection of radon on activated carbon[5,6].
- Systems for delay of ^{220}Rn that is released during reprocessing of high-temperature gas-cooled reactor (HTGR) fuels[2,7].

II. Experimental Procedure

Figure 1 shows the experimental set-up. Medically pure air was supplied at the required flow rate and humidity to a bed of activated carbon. The temperatures of the carbon bed and the inlet air temperature were controlled to ±1°C by electrical heating. Humidity was adjusted by diverting all or part of the air through a 75 mm diameter column filled with water and packed to a depth of 0.37 m with 5 mm Raschig rings. The moisture content of the air was determined by diverting the air through a silica gel trap and measuring the weight gain. Before commencement of most experiments, the activated carbon was conditioned by passing dry air through the bed for 16 hours. In a few experiments, the bed was heated to 60°C and evacuated overnight. Except where indicated, experiments were conducted at standard conditions:- superficial velocity = 0.087 m s^{-1}, temperature = 25°C, relative humidity = 0%, weight of carbon = 50 g and column diameter = 17 mm.

At the beginning of each experiment, air was momentarily diverted through a bed containing 200 g of high grade (about 30% U) uranium ore, resulting in the injection of a sharp pulse of radon into the carbon bed. Typically, about 0.5 μCi of ^{222}Rn was extracted from the ore bed with each milking. Zinc sulfide, α-scintillation flow cell detectors located at the inlet and outlet of the adsorption bed monitored both the pulse input and the subsequent elution of radon from the bed. Hold-up times on the activated carbon varied from about 30 min to 24 h. Counts from the outlet detector were integrated using a ratemeter with a time constant of 40 s and graphically recorded. The data from the chart recorder were punched on cards for processing by a computer.

Five types of activated carbon were tested for their efficiency in adsorbing radon. Variables investigated included air velocity (0.002-0.3 m s^{-1}), temperature (0-55°C), relative humidity (0-100%), bed depth (0.09-0.9 m) and column diameter (17-75 mm).

III. Flow Cell Detectors

The design of the radon flow cell detectors is shown in Figure 2. The detectors were a modified version of a scintillation cell used in the analysis of ^{226}Ra by emanation of ^{222}Rn. The cells, machined from Lucite (trademark of E.I. du Pont de Nemours & Co. Inc.), had internal volumes of 165 mℓ, and could be easily dismantled for cleaning or decontamination. A central Lucite baffle directed the flow to prevent short-circuiting and to minimise dead regions within the cell. All internal surfaces including the Lucite top and baffle were coated with a thin layer of high purity ZnS(Ag) scintillant. The coating was applied by greasing all surfaces lightly with vacuum grease and adding a few grams of ZnS(Ag) powder. The scintillant was then tumbled in the cell until a uniform surface coating was obtained. Excess powder was removed from the cell. Besides directing the flow, the central baffle improved the counting geometry by reducing the average path length that an α-particle could travel before striking a surface coated with scintillant. The flow cell was sealed by O-rings and placed, without optical coupling, on top of the photo-multiplier tube. The whole assembly was housed in

a light-tight enclosure. When freshly coated with scintillant, the background of the detectors was less than one count per minute while the efficiency for detection of radon and its α-emitting daughters was over 90 per cent.

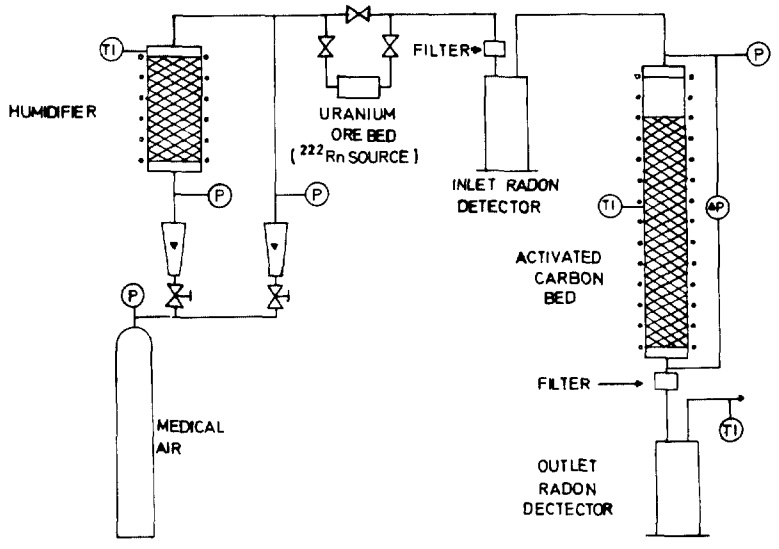

Figure 1. Experimental set-up.

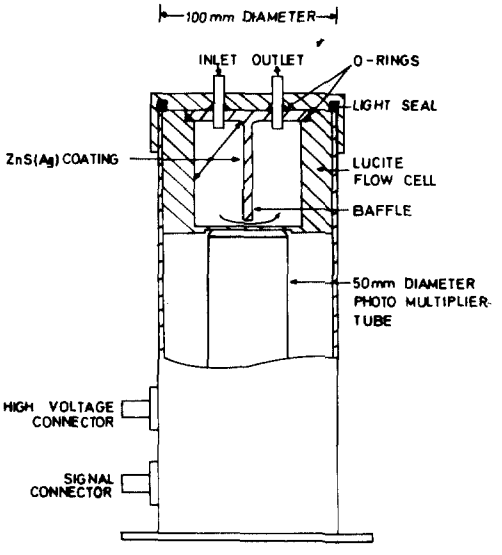

Figure 2. Radon flow cell detector

The inlet of each flow cell contained a glass fiber filter (Whatman GF/B) to remove any radon daughters from the gas stream. Nevertheless, ^{218}Po (RaA) was formed during passage of radon through the flow cell and some was deposited within the cell. The extent of deposition of radon daughters was determined by measuring the rate of decrease in the count rate following passage of a pulse of radon through the inlet detector. The percentage of ^{218}Po deposited varied from 60 per cent to almost 100 per cent and increased as flow rate was decreased. A computer program was written to convert the count rate from the detector to the radon concentration by taking account of the continual deposition and decay of ^{218}Po and the subsequent ingrowth of ^{214}Po. The efficiency of detection of the β-emitter ^{214}Bi was assumed to be zero.

IV. Mathematical Analysis

There are two conventional methods of analysing chromatographic adsorption data. The first approach, borrowed from distillation theory, assumes that a column can be divided into a number of stages of equal volume in which equilibrium always exists between the fluid and the adsorbent. The second approach acknowledges that equilibrium is never actually reached at any point in the column and explains performance in terms of the rate of diffusion and other mass transfer processes. Most descriptions of chromatographic separation rely on the equilibrium stage concept and accordingly this approach is adopted here. The response of N equilibrium stages to a change in concentration of adsorbing species can be determined by solving N first order differential equations that describe the mixing on each stage. For a pulse input in the adsorbing species and assuming a linear isotherm, the elution curve is[8,9]

$$C = \frac{N^{N} T^{N-1} e^{-NT}}{(N-1)!} \qquad (1)$$

where T is dimensionless time normalised to the mean residence time, τ; $T = t/\tau$; and C is dimensionless concentration normalised so that $\int_0^\infty C\, dT = 1$. The mean residence time is given by

$$\tau = \frac{k_a m}{F} \tag{2}$$

where F = flow rate ($m^3(STP)s^{-1}$), k_a = dynamic adsorption coefficient ($m^3(STP)kg^{-1}$) and m = mass of adsorbent in bed (kg). Equation (1) is asymmetric for small N and the maximum in the elution curve occurs at[2]

$$T_{max} = \frac{F\, t_{max}}{k_a\, m} = \frac{N-1}{N} \tag{3}$$

For large N, Equation (1) approaches the Gaussian distribution[10]

$$C = \sqrt{\frac{N}{2\pi}}\; e^{\frac{-N\,(T-1)^2}{2}} \tag{4}$$

and the models based on equilibrium stage theory and diffusion rates coincide.

In practice, the dynamic adsorption coefficient can be determined from the mean residence time or, more simply, from the maximum in the elution curve using Equation (3). A number of methods have been proposed to determine the number of theoretical stages including moment analysis, calculation of the variance, the ratio of peak height to area and the method of tangents[11, 12]. One of the simplest yet accurate methods is to measure the width of the elution curve half-way up the peak ($\Delta t_{\frac{1}{2}}$). Peak widths were determined numerically from Equation (1) and found to satisfy the following relation,

$$\left(\frac{t_{max}}{\Delta t_{\frac{1}{2}}}\right)^2 = 0.180\, N - 0.194 \tag{5}$$

Since the number of theoretical stages depends on column length (L) and the diameter of the packing (d_p), the HETS and the reduced height of a theoretical plate (h) are frequently quoted as indices of column performance[13]. These terms are defined by the equation,

$$h = \frac{HETS}{d_p} = \frac{L}{N\, d_p} \tag{6}$$

V. Results and Discussion

Shape of the Elution Curves

The radon elution curves were processed by computer to determine the dynamic adsorption coefficient from Equation (3) and the number of theoretical stages from Equation (5). For the packed beds used in these experiments, the number of theoretical stages generally varied between ten and one hundred. The theoretical elution curves were calculated from Equation (1) and compared with the experimental curves.

Figure 3 compares a series of experiments using varying bed depths of Pittsburgh PCB activated carbon. In general, the experimental elution curves fitted the theoretical curves quite closely even when the number of theoretical

stages was so low that the asymmetry in the elution curves was obvious. A slight degree of tailing was noted in the experiments using Sutcliffe-Speakman type 207C activated carbon.

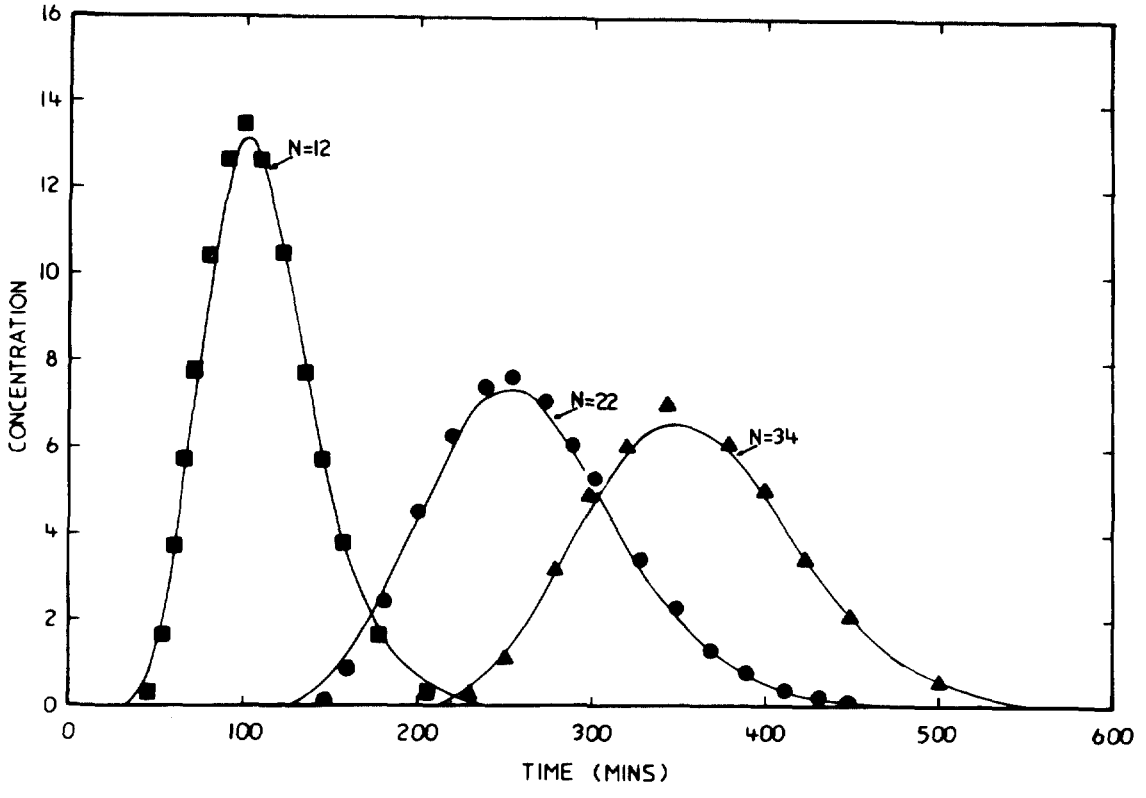

Figure 3. Shape of elution curves.

Air Velocity

As expected, the dynamic adsorption coefficient was found to be independent of air flow rate. Figure 4 shows the effect of superficial air velocity on the HETS for Sutcliffe-Speakman type 207C activated carbon. The minimum HETS was about four times the particle diameter. For velocities above 0.05 m s^{-1}, the HETS increased linearly with velocity.

The shape of Figure 4 agrees with the van Deemter equation for the effect of carrier gas velocity on HETS[14].

$$HETS = A + \frac{B}{u_s} + C\,u_s \qquad (7)$$

where u_s is the superficial gas velocity. A, B and C are, respectively, the coefficients due to eddy diffusion, longitudinal diffusion and resistance to mass transfer which occurs primarily within the adsorbent particle. The value of the constants in Equation (7) that give the best fit to the experimental data are $A = 2.7 \times 10^{-3}$m, $B = 7.3 \times 10^{-6} m^2 s^{-1}$, $C = 0.12$ s. For Sutcliffe-Speakman 207C carbon, Equation (7) can be expressed in dimensionless form as,

$$h = \frac{HETS}{d_p} = 2.2 + \frac{0.73}{Pe} + 0.84\,Pe \qquad (8)$$

where Pe = Peclet number based on superficial velocity ($d_p u_s/D$) and D = diffusion coefficient of adsorbate ($D \sim 10^{-5} m^2 s^{-1}$ for radon). The constants in Equations (7) and (8) are similar to published data for other noble gases[2, 12, 13, 15].

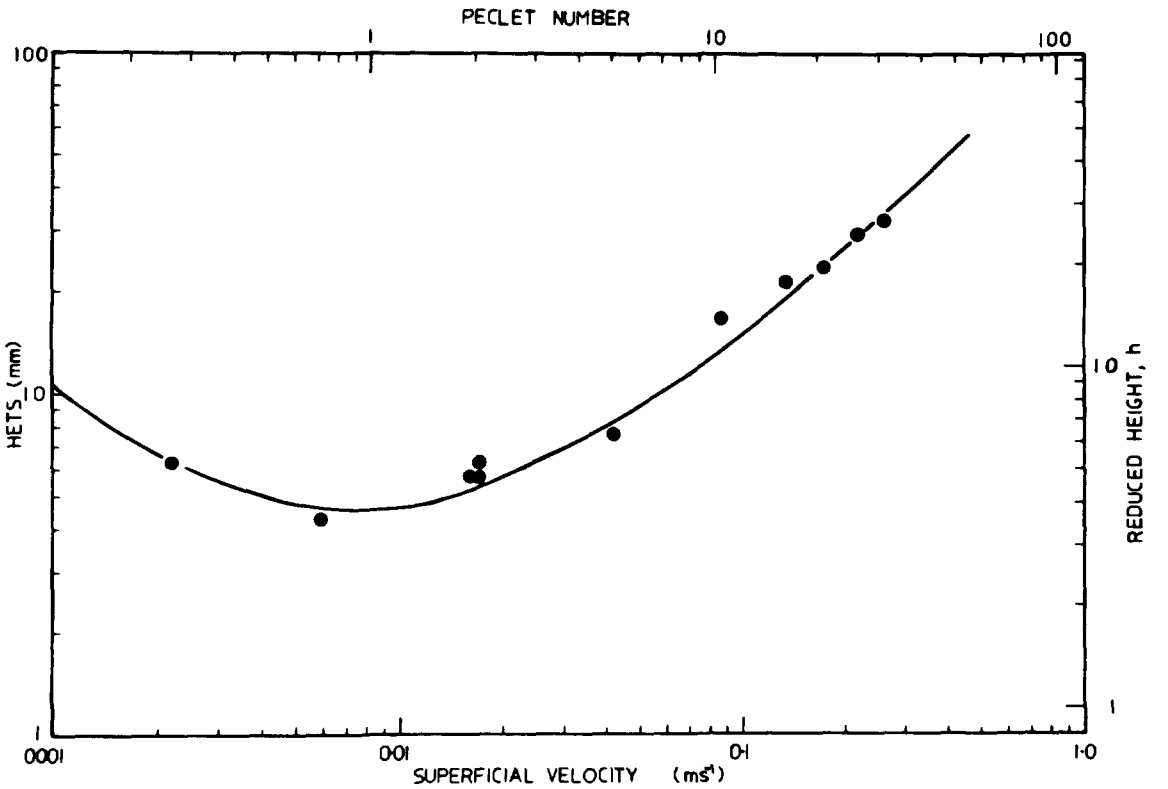

Figure 4. Effect of superficial velocity on HETS (temperature = 25°C)

Temperature

Figure 5 shows that within the temperature range 0-55°C the dynamic adsorption coefficient follows the Arrhenius equation. The calculated heat of adsorption is 6.9 kcal mol^{-1} (29 kJ mol^{-1}) which compares well with values in the range 6.1-7.1 kcal mol^{-1} (26-30 kJ mol^{-1}) reported in the literature[1, 2].

Figure 6 shows the effect of temperature on HETS for Sutcliffe-Speakman type 207C carbon at constant molar flow rate. The HETS increased with temperature in a similar way to that previously reported for adsorption of krypton and xenon on activated carbons[13]. The theoretical effect of temperature on HETS is complex since the effects due to changes in the diffusion coefficient, gas velocity and the dynamic adsorption coefficient often act in different directions[11]. The data in Figure 6 correspond to the case in which mass transfer makes the major contribution to HETS. In this case, for a rise in temperature, the diffusion coefficient increases thus tending to decrease the HETS, whereas the increase in gas velocity and the fall in the dynamic adsorption coefficient tend to increase the HETS. The biggest effect is caused by the change in dynamic adsorption coefficient since this affects the relative times that the adsorbing species spends in the adsorbed state and undergoing mass transfer. Overall the performance should improve (i.e. the HETS should fall) as temperature is decreased[11].

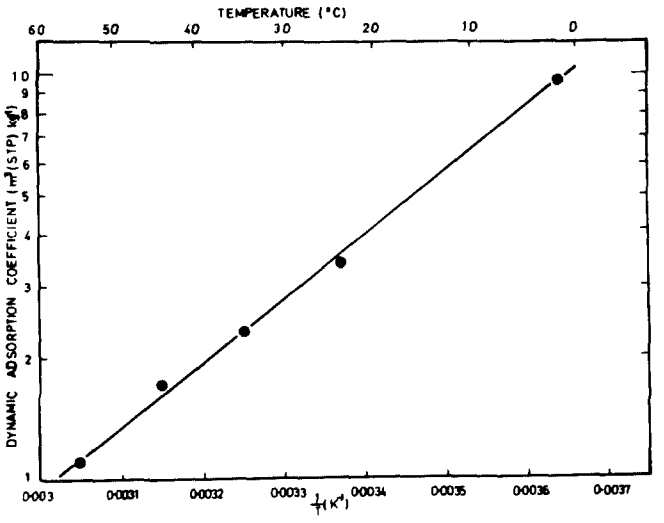

Figure 5. Temperature dependence of the dynamic adsorption coefficient

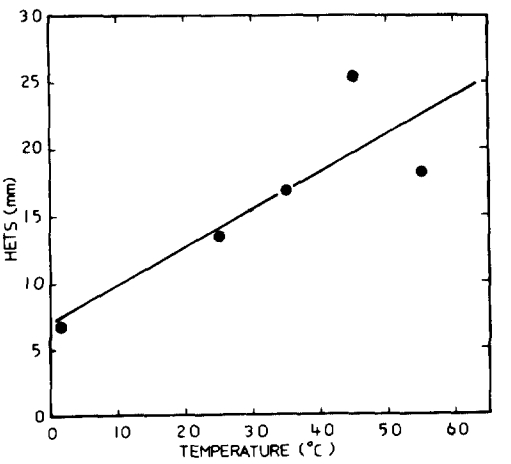

Figure 6. Effect of temperature on HETS

Type of Carbon

A comparative study was made of five commercial grades of activated carbon at the same superficial velocity (0.087 m s^{-1}) and otherwise identical conditions. There was a wide variation in performance as shown in Table 1. The measured dynamic adsorption coefficients ranged from 3.53-5.69 $m^3(STP)kg^{-1}$ compared with values ranging from 0.90-7.50 $m^3(STP)kg^{-1}$ in the published literature[1,2]. Figure 7 shows a positive correlation between the dynamic adsorption coefficient and specific surface area. This is in contrast with the results of Kovach[16] for adsorption of krypton and xenon on activated carbon where the dynamic adsorption coefficient passed through a maximum at a surface area of 900 m^2g^{-1}

Table I. Properties and performance of activated carbons

Type	Source	Shape	Mass Mean Diameter (mm)	Surface Area (N_2, BET) (m^2g^{-1})	k_a $m^3(STP)kg^{-1}$	HETS (mm)	h
Sutcliffe-Speakman 207C	Coconut shell	flakes	1.2	1000	3.53	14.9	12.4
Norit RFL3	Peat	extruded cylinders	4.7	1150	4.61	66.9	14.2
Norit RL111	Peat	extruded cylinders	4.7	1200	4.66	67.9	14.4
Ultrasorb SC2	Coconut shell	chips	0.7	1200	5.00	5.6	8.0
Pittsburgh PCB	Coconut shell	flakes	2.5	1300	5.69	22.9	9.2

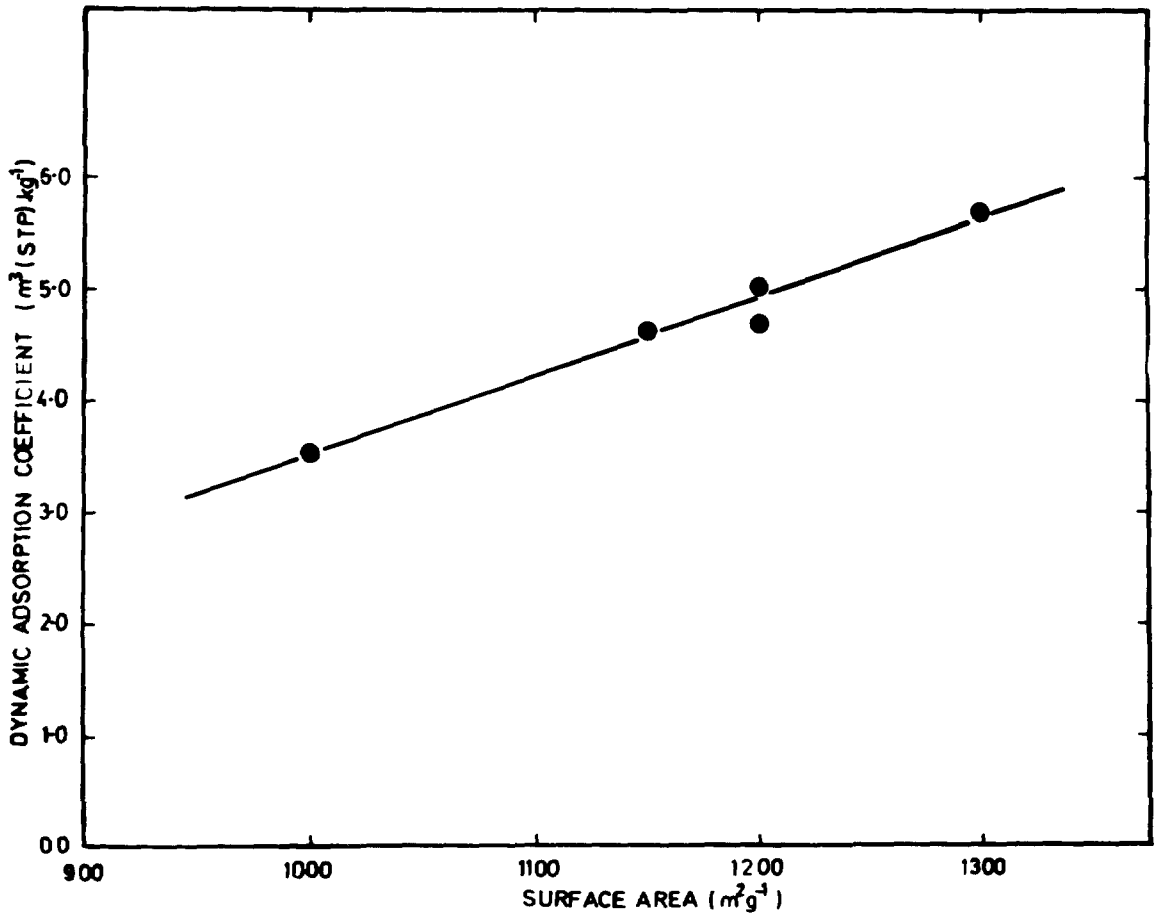

Figure 7. Relation between surface area and dynamic adsorption coefficient

Particle size is the most significant factor affecting the HETS. There appears to be a residual correlation between reduced height of a theoretical stage and both particle diameter and k_a but these effects are difficult to unravel. Prediction of k_a using Equation (8), which strictly only applies to Sutcliffe-Speakman 207C carbon, gives reasonable agreement with the experimental data except for the two Norit carbons. For these extruded cylindrical carbons it is difficult to define an effective diameter for use in the Peclet number, and the predicted values of h using the mass mean diameter are about twice the experimental values.

Bed Height

Four experiments were carried out with bed heights ranging from 90-900 mm but with otherwise identical conditions. The dynamic adsorption coefficient was constant but, as shown in Figure 8, the HETS increased slightly as height was raised. This is a well-known phenomenon in chromatographic columns which has generally been explained in terms of the change in velocity through the bed due to the pressure drop[10, 11]. In the present case, this does not appear to be the explanation since the pressure drop was only 1 kPa per meter of packing. A more plausible explanation for the deterioration in performance as bed height is raised is the progressive increase in channeling in the area of high voidage near the wall. This effect has been observed in other mass transfer equipment and can be remedied in very deep beds by installation of redistributors at regular intervals along the column.

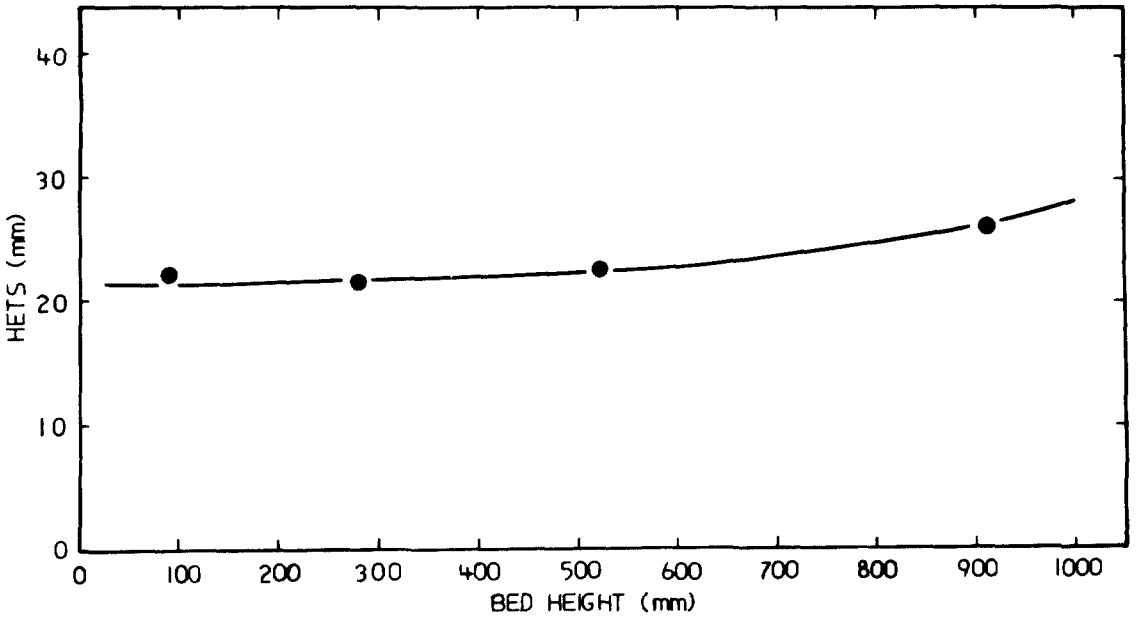

Figure 8. Effect of bed height on HETS (Pittsburgh PCB carbon, temperature = 25°C, superficial velocity = 0.087 m s^{-1})

Column Diameter

A reduction in performance with increase in diameter of chromatographic columns has been reported by many workers and is usually attributed to an uneven flow profile across the column[11]. To determine the effect of column diameter on performance, three experiments were conducted with column diameters ranging from 17 to 75 mm at constant superficial velocity. Each column was carefully packed to the same bulk density (0.47 kg ℓ^{-1}) with Sutcliffe-Speakman 207C activated carbon. The experimentally measured HETS was 5.7 mm for both 17 mm and 38 mm diameter columns and slightly higher (6.4 mm) for the 75 mm column. This variation in HETS was probably within experimental error and these experiments do not indicate a significant effect of column diameter on performance.

Humidity

The effect of water vapor on radon adsorption was studied in two series of experiments. In the first series, the activated carbon bed was first equilibrated with water vapor by passing humidified air through the bed at the test conditions for 16 hours. When equilibrated in this way, the performance of the bed was satisfactory at low relative humidities (<15%) but deteriorated rapidly for higher humidities. The dynamic adsorption coefficient was reduced to 50 per cent of its initial value at 30 per cent relative humidity. The reduction in k_a was matched by a corresponding rise in HETS. A few experiments were carried out at 100 per cent humidity but the retention time was too low to be of practical use. There was considerable scatter in the results of these experiments and local condensation of water was suspected.

In the second series of experiments, humidified air was passed into a dry bed at a temperature of 25°C and a superficial velocity of 0.087 m s^{-1}. Figure 9 shows that the dynamic adsorption coefficient decreased by 30 per cent for an increase in relative humidity from 0-100 per cent. This relatively small effect is explained by the observation that the radon penetrates the bed at a faster rate than water

vapor. Hence, for most of its travel, the radon passes through a dry bed. Near the inlet, the combined effects of temperature rise due to the heat of adsorption of water and the competition with water vapor for active sites tends to reduce the dynamic adsorption coefficient for radon. A computer program is being developed to solve the equations for heat and mass transfer during adsorption of water vapor on activated carbons. Initial results suggest that the effect of temperature rise on k_a is more important than co-adsorption of water vapor.

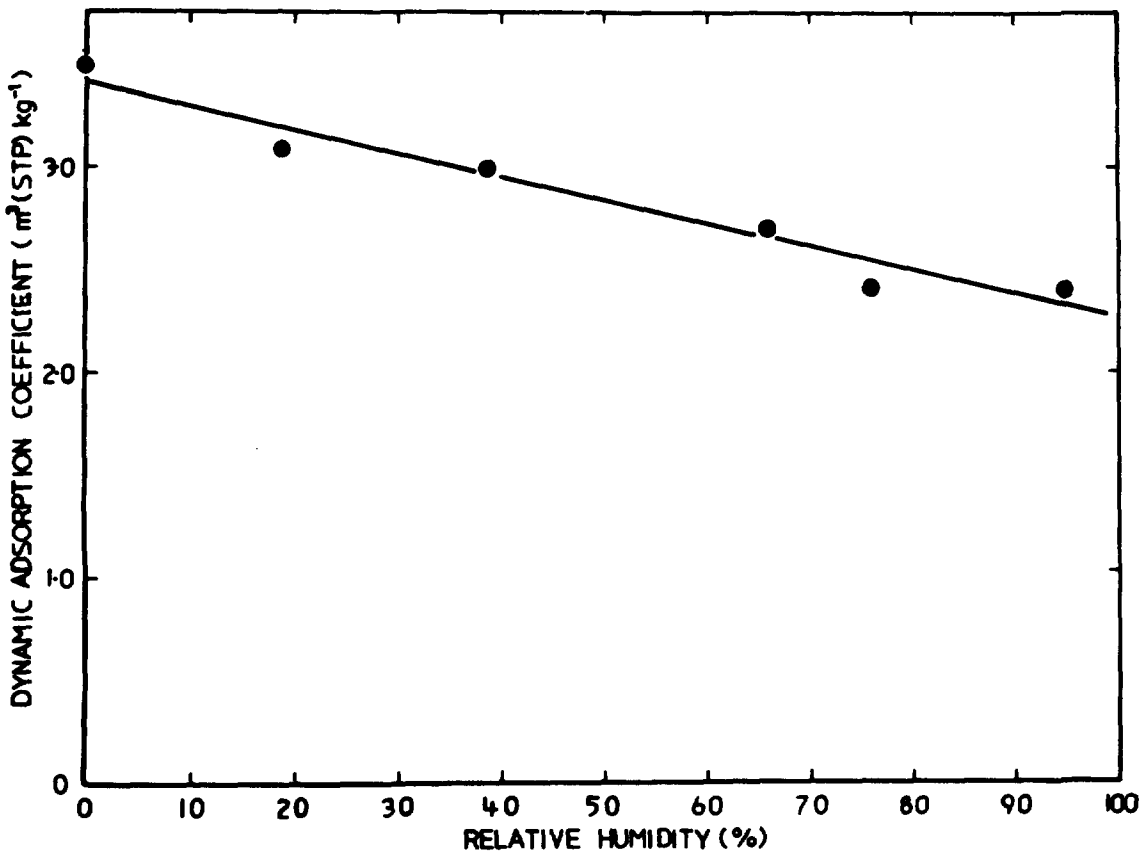

Figure 9. Effect of humidity on the dynamic adsorption coefficient (Sutcliffe-Speakman 207C carbon)

The results reported here are in contrast to the work of Thomas[4] who reported that deterioration in performance of gas mask canisters was most marked when the activated carbon was initially dry. The canister tested by Thomas had a diameter of 0.1 m and a depth of only 31 mm so inlet effects, particularly the sharp initial rise in temperature, would be expected to dominate under these conditions.

Ageing and Regeneration

The activated carbon bed was usually regenerated between experiments by passing dry air through the bed at a superficial velocity of 0.1 m s^{-1} for 16 hours. In a few cases the bed was heated to 60°C and evacuated overnight. This did not improve the adsorption properties of any of the carbons with the exception of Sutcliffe-Speakman type 207C where a slight increase in k_a was observed. Many experiments were conducted with the same carbon bed over several months without deterioration in performance due to ageing.

VI. Application of Results

Since the mass of radon adsorbed on an activated carbon bed for all practical cases is infinitesimal, the performance of a bed is independent of radon concentration and its capacity is determined by the total volume of air that passes through it. In most practical instances, the radon enters the bed as a step change in concentration rather than as the radon pulse used in these experiments. The response to a step change can be simply calculated by integrating the elution curve for a pulse input (Equations (1) or (4)).

For optimum performance, a radon adsorption bed should be sufficiently deep (at least 0.2 m is suggested) so as to contain a large number of stages and minimise broadening of the breakthrough front. The superficial velocity should ideally be in the range 0.002-0.02 m s^{-1}, which will minimise the HETS (see Figure 4) and ensure a low pressure drop. Unfortunately these requirements are not always consistent. This can be seen by expressing Equation (2) in the form,

$$\tau = \frac{T\, k_a \rho_b\, L}{273\, u_s} \qquad (9)$$

where ρ_b = bulk density of the carbon bed, typically about 450 kg m^{-3}. Substituting k_a = 5 m^3(STP)kg^{-1} at T = 298 K in this equation gives

$$\tau = \frac{2500\, L}{u_s} \quad (s) \qquad (10)$$

For the recommended limits, L = 0.2 m and u_s = 0.02 m s^{-1} then τ = 7 h. This means that, unless the bed is designed for a retention time of 7 h or longer, some departure from optimum conditions must be made. In practice, the velocity should be increased rather than the column length reduced because this results in a larger number of theoretical stages.

The design of an activated carbon adsorption process to remove radon from underground mine air was considered by Arthur D. Little Inc.[1]. This design was based on k_a = 4 m^3(STP)kg^{-1} which is consistent with the results reported here after allowing for the effects of humid air on performance. A sharp breakthrough front was assumed and no allowance was made for broadening due to a finite number of stages. The equipment was designed to process 2.36 $m^3 s^{-1}$ (5000 SCFM) at a bed superficial velocity of 0.4 m s^{-1}. For these conditions, the HETS would be approximately 50 mm (see Figure 4) and the bed depth of 0.82 m would be equivalent to only 16 theoretical stages. Broadening of the breakthrough front would be significant and the capacity of the bed would be reduced accordingly. Even with optimistic assumptions, the study found that removal of radon from underground mine air was not competitive with conventional forced ventilation on economic grounds. The major cost was not the carbon adsorber itself but that of ancillary equipment such as blowers, heat exchangers and heating costs associated with thermal regeneration to desorb radon from the exhausted bed. If a simple and cheap method of bed regeneration were devised, adsorption on activated carbon could become a feasible method of removing radon from mine air.

Thomas[4] has demonstrated that portable canisters containing activated carbon can provide short-term protection (up to 1 h) from exposure to very high radon concentrations such as might occur in unventilated mine stopes. The breakthrough data presented by Thomas have been reanalysed to determine the dynamic

adsorption coefficient and values ranging from 3.8-5.7 $m^3(STP)kg^{-1}$ at room temperature have been estimated for the most effective carbon tested[1, 2]. The Mil Army gas mask canister has a depth of only 31 mm which violates the design criteria discussed above. As a consequence, some breakthrough of radon occurs after a very short interval and this canister is not recommended. The Scott-Acme canister has a greater capacity, and being longer (15 cm),it is a more satisfactory design.

Activated charcoal traps are frequently used to collect radon for analytical purposes. Two common applications are atmospheric sampling for ^{222}Rn in the vicinity of uranium mines and mills, and determination of ^{226}Ra in solutions by ingrowth and subsequent de-emanation of ^{222}Rn[5, 6]. In most applications it is recommended that the activated carbon traps be cooled with liquid nitrogen or dry ice. Calculations of adsorber capacity based on the mass of carbon and the volume of air that is passed through the trap frequently show that it is not essential to cool the traps, although in some cases the geometry of the bed needs to be modified. Adsorption of radon at ambient temperatures would simplify procedures particularly in situations that require field work.

Another possible application for activated carbon is the removal of ^{220}Rn from the off-gas stream during reprocessing of HTGR fuel[2, 8]. Since ^{220}Rn has a half-life of only 56 s, only 20 minutes is sufficient for essentially complete retention. Activated charcoal has 10-20 times the adsorptive capacity of molecular sieves and about 200 times that of silica gel[1, 2]. As with other applications for activated carbon, the major disadvantage is the fire hazard.

VII. Conclusions

Over the temperature range, 0-55°C, the dynamic adsorption coefficient for radon on activated carbons with specific surface areas (S) in the range 1000-1300 m^3g^{-1} can be estimated from the equation

$$k_a(m^3(STP)kg^{-1}) = (0.0070S - 3.51)e^{-\frac{6.9 \times 10^3}{RT}} \quad (11)$$

The presence of water vapor in air decreases the dynamic adsorption coefficient. For an initially dry bed of activated carbon at ambient temperature, the dynamic adsorption coefficient decreases by about 30 per cent for an increase in relative humidity from 0-100 per cent. If the bed is allowed to equilibrate with saturated air, the adsorptive capacity is too low to be of practical use.

The minimum height equivalent to a theoretical stage (HETS) occurs at superficial velocities in the range 0.002-0.02 m s^{-1}. This minimum value is typically about four times the particle diameter. For superficial velocities above 0.05 m s^{-1}, the HETS is governed by the rate of mass transfer.

References

1. Arthur D. Little, Inc. "Advanced techniques for radon gas removal". USBM Contract Report H0230022 (May 1975).

2. R.D. Ackley, "Removal of radon-220 from HTGR fuel reprocessing and refabrication off-gas streams by adsorption". ORNL-TM-4883 (April 1975).

3. J.W. Thomas, "Radon adsorption by activated carbon in uranium mines". Proceedings of Noble Gases Symposium, p.637-646, Las Vegas, Nevada (September 1973).

4. J.W. Thomas, "Evaluation of activated carbon canisters for radon protection in uranium mines". HASL-280 (January 1974).

5. R.L. Blanchard, "An emanation system for determining small quantities of radium-226". Public Health Service Publication No. 999-RH-9, Washington D.C. (November 1964).

6. H.F. Lucas, "Alpha scintillation radon counting". Workshop on Methods for Measuring Radiation in and around Uranium Mills, Albuquerque, New Mexico (May 1977).

7. F.A. Hohorst, "Containment of ^{220}Rn via adsorption on molecular sieves for HTGR-OGCS". ICP-1114 (May 1977).

8. O. Levenspiel, "Chemical Reaction Engineering". John Wiley & Sons Inc. New York (1964).

9. D.P. Siegwarth, C.K. Neulander, R.T. Pao and M. Siegler, "Measurement of dynamic adsorption coefficients for noble gases on activated carbon". Proceedings of 12th AEC Air Cleaning Conference, p.28-46, Oak Ridge, Tennessee (August 1972).

10. A.I.M.Keulemans, "Gas chromatography". Reinhold Publishing Corp., New York (1957).

11. A.B. Littlewood, "Gas chromatography". Academic Press, New York (1970).

12. D.W. Underhill, "An experimental analysis of fission-gas hold-up beds". Nucl. Appl. & Tech. Vol. 8, 255-260 (1970).

13. D.W. Underhill, "Dynamic adsorption of fission product noble gases on activated charcoal". NYO-841-8 Harvard Air Cleaning Laboratory (1967).

14. J.J. van Deemter, F.J. Zuiderweg, and A. Klinkenberg, "Longitudinal diffusion and resistance to mass transfer as causes of nonideality in chromatography". Chem. Eng. Sci. Vol. 5, 271 (1956).

15. G. Collard, M. Put, J. Broothaerts and W.R. Goossens, "The delay of xenon on charcoal beds". Proceedings of 14th ERDA Air Cleaning Conference p.947-955 Sun Valley, Idaho (August 1976).

16. J.L. Kovach, E.L. Etheridge, "Mass and heat transfer of krypton-xenon adsorption on activated carbon". Proceedings of 12th AEC Air Cleaning Conference, p.71-85, Oak Ridge, Tennessee (August 1972).

DISCUSSION

TADMOR: Dr. Levins, as you rightly mentioned, radon is a problem in the mining of uranium, but it may be also a long term problem from the long term release of radon from tailings and other residual materials from mining. Do you have any data, or would you venture to make some predictions, on the adsorption of radon on soil and underground material which may be used to cover the tailings produced in mining or milling of uranium?

LEVINS: We haven't a lot of evidence on the adsorption of radon on soil materials. My general observation would be that it wouldn't be very strong. There is one exception: silica, that may appear in tailings, may adsorb the radon weakly, but I don't think it would be a significant factor in retarding the release of radon from a mine site or tailings pile.

DEVELOPMENT OF A CRYOGENIC KRYPTON-SEPARATION SYSTEM FOR THE OFFGAS OF REPROCESSING PLANTS

R. v. Ammon, H.-G. Burkhardt, E. Hutter and G. Neffe
Kernforschungszentrum Karlsruhe GmbH, Federal Republic of Germany

Abstract

The concept of cryogenic rare gas separation from reprocessing offgas pursued at present at the Kernforschungszentrum Karlsruhe (KfK) is discussed and compared with other offgas purification flowsheets. The KfK concept includes: separation of O_2 and residual NO_x by catalytic reduction with H_2, adsorptive retention of H_2O, CO_2, NH_3 etc. and cryogenic distillation of first N_2-Kr-Xe, then Kr-Xe mixtures. Some features pertinent to this flowsheet which were studied experimentally either on a laboratory or semiworks scale, are described including the following: desublimation of Xe in the first column, coadsorption of Kr at and its selective desorption from the adsorption bed, purification of the Xe product, poisoning of the reduction catalyst and methanization of CO_2. It is shown that all of these features, despite being capable of causing malfunctions of the process, can be controlled by proper process design and operational conditions in a way not to impair with a good Kr decontamination factor.

I. Introduction

Plans for retention of the fission gas Kr from the offgas of the future large German reprocessing plant as well as of the existing small plant WAK (Wiederaufarbeitungsanlage Karlsruhe) prefer a cryogenic distillation scheme. The reason is the long experience with such a process in the industrial production of rare gases in air liquefaction[1].

Two essential differences between the rare gas-oxygen mixtures in air liquefaction plants and reprocessing offgases demand for modifications of the process:

- the mole ratio Kr/Xe in fission gas (0,103) which is almost reciprocal to the ratio in air (13,1); the resulting higher Xe-concentrations enhance the problem of Xe freeze-out;
- the radioactivity of Kr-85 resulting in the radiolytic ozone formation from O_2.

Depending on the risks one places on these differences the existing or planned Kr retention units show different flowsheets (fig. 1)[2]. At the I.N.E.L. (U.S.A.) [3] and at the C.E.A. (France) [4] the complete offgas including O_2 is liquefied in the first column. Here the risk of ozone formation is accepted, but freeze-out of Xe is decreased because of improved solubility in O_2 compared to N_2. Further enrichment of Kr is achieved either by batch distillation of the three-component mixture O_2-Kr-Xe in the second column (I.N.E.L.) or by catalytic reduction of O_2 with H_2 between the two columns and

subsequent distillation of Kr-Xe (C.E.A.).

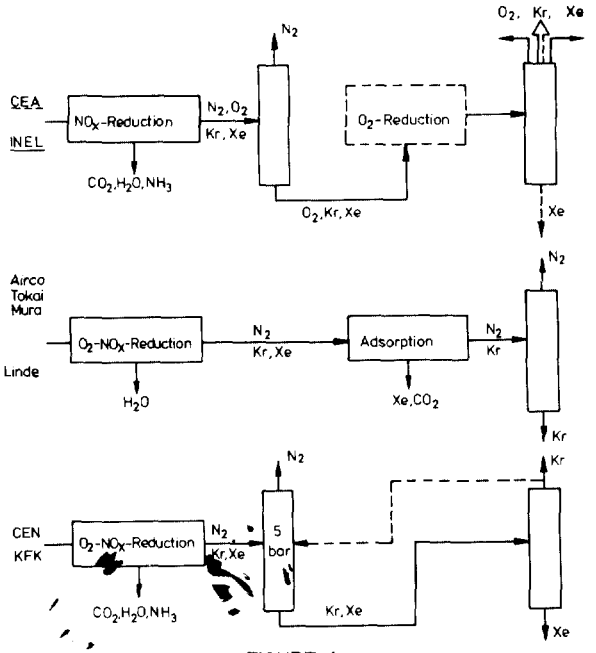

FIGURE 1

Different flowsheets for the retention of Krypton from the offgas of LWR-reprocessing plants

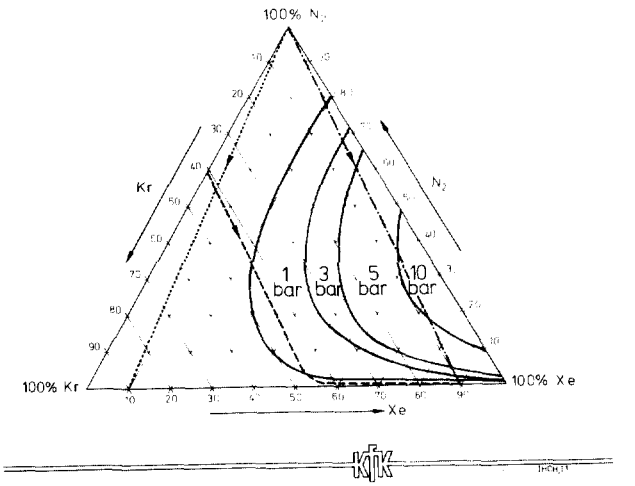

FIGURE 2

Pressure dependence (ideal behavior) of the two-phase area solid-liquid in the phase diagram N_2-Kr-Xe and course of bottom product concentrations during start-up operation of column

- ·-·-without additional Kr
- - - additional Kr before operation } Different operation modes
- ····· with Kr recycle

Both risks are circumvented by proposals of Linde (Germany)[5] and by Airco (U.S.A.) for the Japanese Tokai Mura plant[6]: both O_2 and Xe are separated from the offgas before the cryogenic part by catalytic reduction and by adsorption, respectively. Workers at KFA Jülich (Germany) prefer a separation of Xe by freeze-out instead of adsorption[7]. After separation of Xe the cryogenic distillation is simplified to the two-component system N_2-Kr.

In the present concept of KfK[8], similar to the plans of the C.E.N. (Belgium)[9] O_2 is also removed by catalytic reduction, but adsorption of Xe is omitted. Thus the three-component system N_2-Kr-Xe must be distilled in the first column. Whereas N_2 is driven off at the head, Kr and Xe are collected in the bottom of the still. After discontinuous transfer to the second column Kr and Xe are separated into pure products and filled into steel cylinders. The cryogenic part of this concept together with a preceding molecular sieve bed as drying unit was installed on a "cold" semiscale basis (gas throughput 30-50 m^3/h at S.T.P.). These units which bear the names KRETA (Krypton-Entfernungs-Tieftemperatur-Anlage) and ADAMO (Adsorption an Molekularsieben) have been in operation now for 4000 hours. The

design of these units has been described elsewhere[10]. Some of the results gained are reported in the following sections.

II. Features of the KfK Flowsheet and Results

1. Desublimation of Xenon

1.1 Solid-Liquid Equilibrium

The phase diagram of the three-component system N_2-Kr-Xe has a region of limited solubility on the N_2-Xe side. Solid Xe is in equilibrium with N_2-Kr-Xe liquid (fig. 2). This two-phase area decreases on increasing the pressure and thus the temperature. One could therefore prevent Xe from freezing out completely by operating the column at 17-20 bar[11-13]. Because of safety aspects in plants containing large inventories of radioactivity we chose an intermediate pressure of 5 bar which is also familiar practice in air liquefaction.

Fig. 2 also shows the problem of Xe freeze-out during the start-up period of the column: if the fission gas mixture is fed into the column cooled down with liquid nitrogen (at 95 K) one would pass straight through the critical area (dot-dashed line). This situation can be avoided, if the column is filled with a N_2-Kr mixture before the fission gas feed is opened. In this case the stationary bottom concentration is approached first on a straight line, then, after opening the bottom product transfer line to the second column, on a curved line (dashed line). The critical area is not intersected. Alternatively, one can also raise the Kr/Xe ratio to or near that of the air by means of an additional Kr feed. In the second Kr separation unit at Karlsruhe being in the planning state now for the offgas of the WAK plant a Kr recycling loop from the top of the second column to the first column possibly will be installed (see fig. 1)[14]. In this case one would be on the safe side in all parts of the column (dotted line in fig. 2).

We have tested all three versions in the KRETA campaigns and confirmed the expectations: whereas in the first version we had serious malfunctions of the column because of Xe freeze-out, we have attained Xe concentrations up to 80 % in the bottom product in the second version without having detected any precipitation of solid Xe.

During unperturbed operation of the column the Kr decontamination factor (DF) at the head was $\geq 10^3$, the upper limit set by the sensitivity of the He ionization detector of our gaschromatographic analysis (100 ppb) and the normal Kr feed concentration of 160 ppm by vol.

1.2 Gas-Solid Equilibrium

More essential than the solid-liquid equilibrium is in our column the gas-solid equilibrium. Due to the construction of the column which is a sieve plate column containing 37 plates with the feed point above the 18th plate (overall height: 8 m) and due to the temperature profile within the column (gas temperature at the feed point: 135 K) we observe desublimation of Xe at the first plate above the feed point (temperature: 95 K) under certain conditions. There solid Xe is not dissolved completely by liquid N_2, but accumu-

lates until the sieve holes are plugged. According to the sublimation pressure curve of Xe (fig. 3) the limiting Xe-concentration in the feed gas at 95 K should be only 80 ppm. In practice we observe a limiting Xe concentration which is higher by almost an order of magnitude. We conclude therefore that the difference is either dissolved by liquid N_2 or carried down the column mechanically in solid form. The aim of our present work is to increase this concentration by increasing the temperature profile in the vicinity of the feed point and by altering the construction of the column interior in that area.

What are the consequences of this result for the rare gas separation from a real offgas ? The offgas most pertinent to our development at the moment is the offgas of the WAK. This offgas consists of 80 - 120 m^3/h at S.T.P. of essentially air containing a maximum of 1600 ppm of Xe at the peak of a dissolution. If continuously fed to a column like ours, it should result in serious plugging after a short time. However, a dissolution of fuel in WAK is essentially completed after two hours followed by a day until the next dissolution starts. We simulated such a feed gas in KRETA (fig. 4) and showed that such a rare gas concentration peak does not lead to any signs of plugging, even if another rare gas peak simulating a dissolution is fed to the column two hours after the end of the first run.

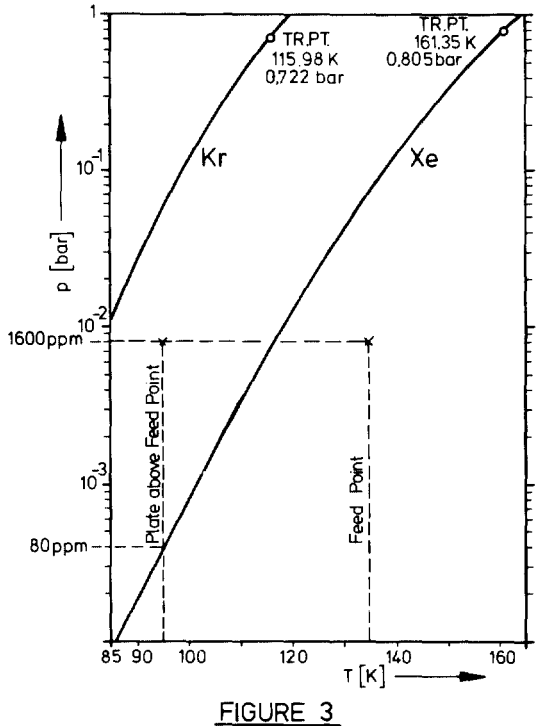

FIGURE 3
Sublimation pressure of Krypton and Xenon

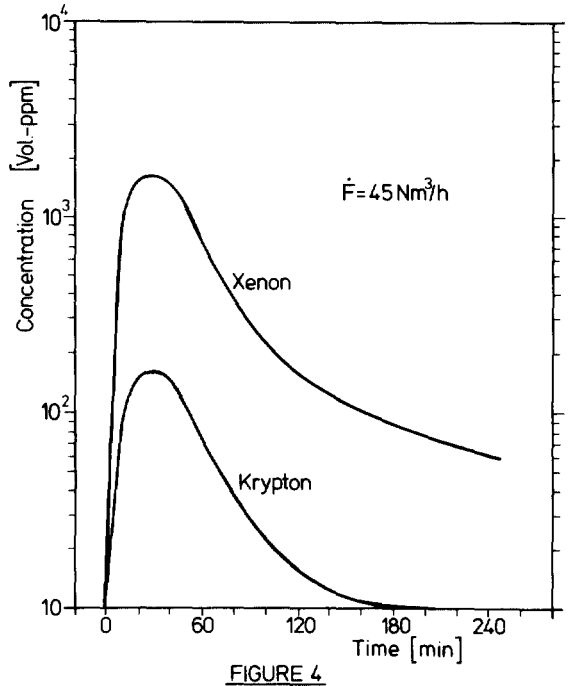

FIGURE 4
Kr-and Xe-concentrations in a simulated offgas of a dissolution at WAK

In the case of a large reprocessing plant where rare gas concentrations probably will be higher and on a more continuous level, this concept would have to be changed, however, unless we can avoid plugging by desubliming Xe by means of modifying the column structure.

2. Ozone Formation

The primary reason for the separation of O_2 in our concept was to prevent excessive ozone formation. However, even during normal operation, not to speak of malfunction of the reduction catalyst traces of O_2 will reach the cryogenic column. Ozone formation rates therefore have to be known. In addition, use of liquid O_2 as solvent for the rare gases in the first cryogenic column is an interesting process alternative in many respects[3]. If one considers this alternative, the safety risks of ozone formation have to be assessed. We have therefore carried out a calculation of the ozone concentration to be expected in the first column considering three process alternatives (table I):

1) The first case is the alternative presently investigated by us in the KRETA pilot plant; it is assumed that 10 ppm O_2 pass the reduction unit.
2) The second case was proposed for the offgas purification system at the WAK[14], called project AZUR. Here the ratio Kr/Xe is raised to that of air by a Kr recycling loop; O_2 again is reduced down to 10 ppm.
3) In the third case, O_2 which is present in the offgas in air concentration (20 %) is not reduced; it is partially (50 %) liquefied thus acting as solvent for the rare gases; Kr is not recycled.

The O_2 and Kr concentration profiles along the column were calculated by a tridiagonalmatrix method[15]. Stationary column operation has been assumed which is attained 700 hours after startup.

The ozone formation rate was calculated according to the equation shown in fig. 5, where an average G-factor of 10 was assumed [16], where ε_{O_2} is the O_2 electron fraction, where the Kr concentration C_{Kr} takes into account the abundancy of Kr-85 in overall Kr (6 %) and where the radiation dose rate is the product of the specific activity of Kr-85 and its average ß-energy. The dimensions of the column considered are typical of the KRETA pilot plant (liquid volume of bottom product: 15 l, and of each of 10 theoretical plates: 1,2 l).

The calculated ozone concentrations in the bottom product are given in table I. Surprisingly the highest value is not obtained in the case of O_2 operation (case 3), but with 10 ppm O_2 in the feed gas (case 1), whereas in the Kr recycle mode (case 2) it is lowest. The explanation is found in the different transfer rates of the bottom product; whenever this rate is high, the residence time of O_2 and Kr in the column is short and thus the ozone formation rate is low. This is particularly true for cases 2 and 3. In case 2 the effect of high Kr concentration is even overcompensated.

Generally, the calculated ozone concentrations are very low and presumably beyond a critical concentration[17,18]. The calculation

Flowsheet		1 "KRETA"	2 Kr-Recycle	3 O_2-Liquefaction
Feed Composition (N_2 Carrier Gas)	Kr	500 Vol.-ppm	5 Vol.-%	500 Vol.-ppm
	Xe	5000 Vol.-ppm	5000 Vol.-ppm	5000 Vol.-ppm
	O_2	10 Vol.-ppm	10 Vol.-ppm	20 Vol.- %
Transfer Rate of Bottom Product [l/h]		0,56	3,98	8,41
Krypton-Inventory	[l]	2,24	21,2	0,06
	[Ci]	$1{,}14 \cdot 10^5$	$1{,}08 \cdot 10^6$	$3{,}06 \cdot 10^3$
Ozone-Concentration [Mol-ppm] (Bottom)		170	8,2	53

Table I

Ozone formation in the first cryogenic column in different process flowsheets

$$\frac{d[O_3]}{dt} = \frac{G\,[eV^{-1}] \cdot \varepsilon_{O_2}[Mol/Mol] \cdot C_{Kr}[Mol/Mol] \cdot \text{dose rate}\ \ [eV \cdot l^{-1} \cdot s^{-1}]}{N_L\,[Mol^{-1}]}$$

$$\frac{d[O_3]}{dt} = \frac{10 \cdot 10^{-2}\,[eV^{-1}] \cdot \varepsilon_{O_2} \cdot 0{,}06 \cdot C_{Kr} \cdot 8{,}51 \cdot 10^5\,[Ci \cdot l^{-1}] \cdot 3{,}7 \cdot 10^{10}\,[Ci^{-1} \cdot s^{-1}] \cdot 2{,}49 \cdot 10^5\,[eV]}{6{,}02 \cdot 10^{23}\,[Mol^{-1}]}$$

$$\frac{d[O_3]}{dt} = 7{,}8 \cdot 10^{-5} \cdot \varepsilon_{O_2} \cdot C_{Kr}\ [Mol \cdot l^{-1} \cdot s^{-1}]$$

FIGURE 5

Ozone formation rate in cryogenic rare gas mixtures

shows that ozone formation is not a serious problem in cryogenic Kr separation, since it can be controlled by proper design of the process. It must be kept in mind, however, that further build-up of the ozone level may take place in the second column, especially in the Xe product, if an ozone and oxygen reduction step between the columns is not considered (4, 17, 19).

Table I indicates another inherent safety aspect: the inventory of Kr and thus of the activity. It varies by almost three orders of magnitude and is lowest in the O_2 operation mode and highest in the Kr recycle mode.

3. Points of Krypton Leakage Inherent to the Process

The head of the first column is the most important, but not the only point, where Kr is released to the atmosphere. Two additional points are discussed in the following sections.

3.1 Adsorption Unit

A conventional adsorber unit is provided in our pilot plant to dry the feed gas and, lateron, to retain all offgas components which, if present, would freeze out in the cryogenic part, i.e. CO_2, NO_x and NH_3. Some Kr is also adsorbed during this step. Although this coadsorption of Kr is weak at room temperature (20), it would be sufficient to spoil the good column decontamination factor, if it would be released to the atmosphere on regeneration of the adsorber. Therefore a purging step is included in the operation mode of the adsorber bed, where the coadsorbed Kr is selectively desorbed and recycled. This concept led to the design of three adsorber lines each consisting of two beds. The first one is presently filled with 70 kg of silicagel, the second one with 100 kg of molecular sieve type 10A.

Breakthrough (at $c/c_E = 0{,}5$) of Kr (160 ppm by vol.) and Xe (1600 ppm) in 31 m^3/h (S.T.P.) at 5 bar and room temperature takes place after 4.2 and 26.0 minutes, respectively, through the two beds of a line. Desorption curves for Kr labelled with Kr-85 , and Xe using a purge gas stream of 5 m^3/h (S.T.P.) at 1 bar and room temperature are shown in fig. 6. The bulk amount of Kr has been desorbed already after 30 minutes, after 2 hours only 1 %o of the Kr originally adsorbed remains on the beds. If one would stop the purging step at this point, this residual Kr would be released on heating the bed in the regenerating step. It can be shown that a release of 14 %o instead of 1 %o residual Kr would still limit the release to the same amount which is released at the head of the first column at a column decontamination factor of 10^3.

3.2 Xenon Product

The bottom product of the first column after transfer to the second column (packed bed) is separated by distillation into Kr (head product) and Xe (bottom product). This process step is only sensible, if storage volume of radioactive product can be saved. This is possible only, if the inactive Xe can be purified from Kr-85 to such an extent that it can be released to the atmosphere (or utilized commercially). If we postulate again that the amount of Kr-85 released with the Xe product should not exceed the amount released at the head

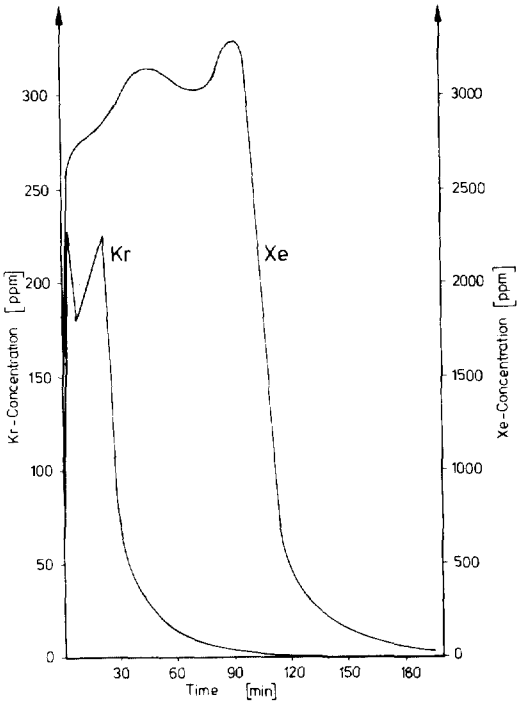

FIGURE 6

Desorption of Kr and Xe from the silica and molecular sieve beds in the pilot plant ADAMO with 5 Nm^3/h N_2 at 1bar and 25°C

head of the first column at a DF = 10^3, then the Kr content of the Xe must be limited to 100 ppm by vol.

This postulate could be fulfilled almost routinely. At the moment, the Kr and Xe products are both collected in steel cylinders by means of a membrane compressor. Lateron, transfer of the products into the cylinders by way of cryogenic pumping will be applied.

4. Catalytic Reduction of O_2 and NO_x

4.1 Poisoning of Noble Metal Catalysts

On the basis of laboratory experiments a Ru catalyst on Al_2O_3 carrier of relatively low specific surface area (9 m^2/g) has been selected as catalyst for the reduction of O_2 and residual NO_x with H_2. From all nobel metals investigated, this catalyst is most resistant to poisoning by iodine and organic phosphorus compounds which are both trace components of reprocessing offgases. The poisoning effect of I_2 was studied with respect to activity and selectivity on a series of Pt, Pd and Ru catalysts. Some of the results are shown in Fig. 7 and 8. The activity of Pt and Pd is definitely reduced by increased loading with I_2. As can be expected, the activity of catalysts of high specific surface is more strongly affected than of

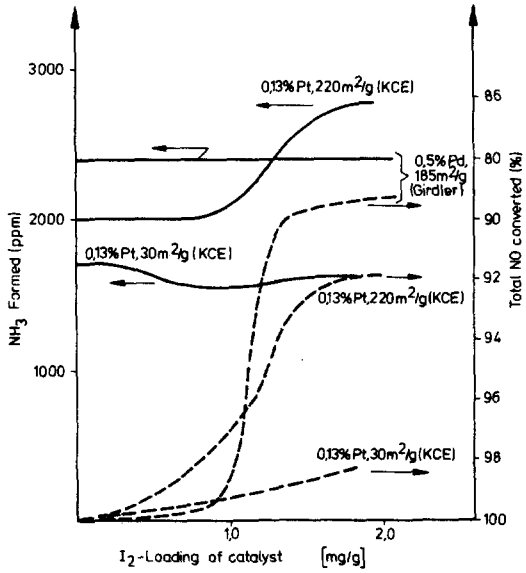

FIGURE 7

Poisoning effect of I_2 on Pt-and Pd-catalysts with respect to activity and selectivity of NO-reduction.
Inlet concentration: 0,75vol-% O_2; 0,5vol.-%NO; 2,75vol.-% H_2;
Space velocity : 5000 h^{-1}; 400 °C.

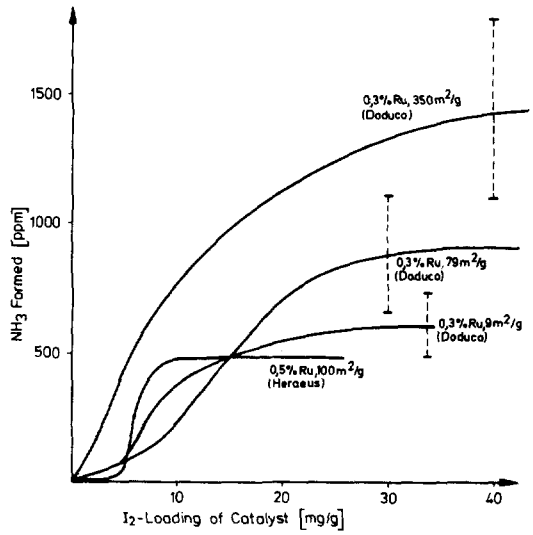

FIGURE 8

Poisoning effect of I_2 on Ru-catalysts with respect to selectivity of NO-reduction.
Inlet concentrations: 0,75Vol-% O_2, 0,5 Vol.-% NO, 2,75Vol.-% H_2;
space velocity: 5000 h^{-1}; 400°C.

types of lower specific surface area. The selectivity which is not good at the beginning (about 40 - 50 % NH_3 formed, the rest N_2), is not affected significantly, however [21].

On the contrary, the activity of Ru catalysts is not influenced even by very high I_2 loadings: under the experimental conditions, NO is reduced throughout to a residual level of $\leq$ 1 ppm. A poisoning effect can only be observed in the selectivity: formation of NH_3 which is very low in the unpoisoned state (22), increases more or less strongly on increasing I_2 loading (fig. 8). Again, the influence of the specific surface area is obvious. The NH_3 formation never reaches the amount produced at Pt and Pd.

Thus, on the basis of these data, further work will be carried out with the Ru catalyst of low specific surface area. It can be shown that in a real offgas the time of operation of such a catalyst bed should not be limited below about one year by iodine poisoning, if an iodine filter with a DF of 10^3 or better is installed before the catalyst.

4.2 Formation of Methane

It is well known that Ru is an active catalyst for the reduction of CO_2 to CO and CH_4 (23). CO_2 is an essential component of the

offgas if air is the carrier gas. In addition, CO_2 is formed, if organic substances are burned on an oxidation catalyst, which is conventional practice in air liquefaction plants. Also, C-14 is set free from the fuel elements predominantly as $^{14}CO_2$. CO and CH_4, if formed at the reduction catalyst, will not be retained at the adsorption bed and will reach the cryogenic column. According to their boiling points (81.7 K and 111.6 K at 1 bar, respectively) they will attain a certain equilibrium concentration there. For two reasons CH_4 formation must be avoided:

- it is a safety hazard in the presence of O_2 (or O_3);
- retention of C-14 will be inhibited.

The reduction of CO_2 by H_2 is governed thermodynamically by the equilibria given in table II (23). Whereas CO is formed preferably at higher temperatures ("water gas" reaction), CH_4 is formed preferably at lower temperatures ("Fischer-Tropsch" reaction).

Table II: Reduction of CO_2 by H_2

I. $CO_2 + H_2 \rightleftharpoons CO + H_2O$

$$Kp^{I} = \begin{cases} 0{,}067 \text{ at } 350\,^{\circ}C \\ 0{,}017 \text{ at } 250\,^{\circ}C \end{cases}$$

II. $CO + 3H_2 \rightleftharpoons CH_4 + H_2O$

$$Kp^{II} = \begin{cases} 2{,}62 \text{ at } 350\,^{\circ}C \\ 3{,}04 \text{ at } 250\,^{\circ}C \end{cases}$$

III. $CO_2 + 4H_2 \rightleftharpoons CH_4 + 2H_2O$

$$Kp^{III} = Kp^{I} \cdot Kp^{II} = \begin{cases} 0{,}18 \text{ at } 350\,^{\circ}C \\ 0{,}05 \text{ at } 250\,^{\circ}C \end{cases}$$

The overall equilibrium constant is the product of both Kp^{I} and Kp^{II} shifting reaction III to the right with increasing temperature. The experimental results show that at temperatures above 400°C substantial amounts of CO, but little CH_4 is formed, whereas at lower temperatures high yields of CH_4 are obtained depending strongly on the H_2-concentration. Thus one requirement for the minimization of CO_2-reduction is to keep the overstoichiometric H_2 amount with respect to

the reduction of O_2 and NO_x as low as possible.

As a matter of fact, the presence of O_2 suppresses the formation of CH_4 drastically, the overall atmosphere still being reducing. If O_2 is added to a gas mixture containing only CO_2 and H_2 in N_2, the formation of CH_4 immediately drops down below the level of detection (20 ppm by gaschromatography). Equilibrium III (table II) is shifted to the left by a decrease of the H_2- and an increase of the H_2O-concentration.

It can be concluded from these results that in a realistic offgas formation of CH_4 at the reduction catalyst can be controlled to such an extent that it poses no serious problems from a safety standpoint.

Acknowledgements

We acknowledge gratefully the assistance of the following coworkers and colleagues carrying out the experiments and calculations: W. Bumiller, G. Franz, E. Hauß, G. Kimmig, G. Knittel and K. Schulz. We also thank E. Henrich, C.H. Leichsenring, R.-D. Penzhorn and W. Weinländer for stimulating discussious.

References

1) Ullmanns Encyklopädie der techn. Chemie, 3. Aufl. (W. Foerst, Hrsg.), Band 6, p. 208, Urban und Schwarzenberg, München-Berlin 1955.

2) R. v. Ammon and H. Beaujean, in "Chemie der Nuklearen Entsorgung" (F. Baumgärtner, Hrsg.), Thiemig-Taschenbuch Bd. 66, 1978.

3) C.L. Bendixsen and F.O. German, ICP-1057 (1975).

4) A. Chesné, J.P. Goumondy, P. Miquel and A. Leseur, CEC-Seminar on Radioactive Effluents from Nuclear Fuel Reprocessing Plants, Karlsruhe 1977, p. 447.

5) R. Glatthaar, Kerntechnik 18, 431 (1976).

6) T. Kon and S. Motoyama, Techn. Committee on Removal, Storage and Disposal of Gaseous Radionuclides from Airborne Effluents, IAEA Vienna 1976.

7) J. Bohnenstingl, M. Heidendael, M. Laser, S. Mastera and E. Merz, IAEA-SM-207/20 (1976).

8) R. v. Ammon, W. Weinländer, E. Hutter, G. Neffe and C.H. Leichsenring, KfK-Nachrichten 7, 63 (1975).

9) L.H. Baetslé and J. Broothaerts, CEC-Seminar on Radioactive Effluents from Nuclear Fuel Reprocessing Plants, Karlsruhe 1977, p. 421.

10) R. v. Ammon, E. Hutter, C.H. Leichsenring, G. Neffe and W. Weinländer, in KfK-2262 (1976), p. 144; Deutsches Atomforum, Reaktortagung 1976, p. 339.

11) R. v. Ammon, W. Bumiller, E. Hutter and G. Neffe, KfK-2570 (1978) p. 242.

12) S. Mastera, J. Bohnenstingl, M. Laser and E. Merz, Brennstoff-Wärme-Kraft 29, 214 (1977).

13) F. Anderle, H. Frey and G. Lerch, Kerntechnik 19, 483 (1977).

14a) H. Gutowsky, W. Haas and A. Patzelt, Deutsches Atomforum, Reaktortagung 1978, p. 441.

14b) H. Beaujean, U. Tillessen, G. Engelhardt and G. Israel, CEC-Seminar on Radioactive Effluents from Nuclear Fuel Reprocessing Plants, Karlsruhe 1977, p. 551.

15) W. Pfeifer and G. Neffe, unpublished.

16) J.F. Riley, ORNL-3176 (1961), p. 33.

17) C.L. Bendixsen, F.O. German and R.R. Hammer, ICP-1023 (1973).

18) E. Karwat and G. Klein, Linde Berichte aus Technik und Wissenschaft Nr. 4 (1950), p. 3.

19) G.E. Schmauch, ASME 74-WA/NE-2 (1974).

20) S. Kitani and J. Takada, J. Nucl. Sc. Techn. 2, 51 (1965).

21) R. v. Ammon, K. Strauch, W. Weinländer and W. Wurster, KfK-2437 (1977)

22) M. Shelef, Catal. Rev. 11, 1 (1975).

23) Ullmanns Encyklopädie der techn. Chemie, 4. Aufl., Band 14 p. 329, Verlag Chemie, Weinheim-New York 1977.